SCIENTIFIC REPORTS

SUBJECT AREAS:
INFLUENZA VIRUS
MECHANISMS OF DISEASE
TRANSCRIPTOMICS
VIRAL HOST RESPONSE

Received
13 October 2012

Accepted
19 March 2013

Published
3 April 2013

Correspondence and requests for materials should be addressed to M.J. (jml8328@126.com)

* These authors contributed equally to this work.

Insights into the increasing virulence of the swine-origin pandemic H1N1/2009 influenza virus

Wei Zou[1]*, Dijun Chen[2,3]*, Min Xiong[3]*, Jiping Zhu[1], Xian Lin[1], Lun Wang[4], Jun Zhang[1], Lingling Chen[3], Hongyu Zhang[3], Huanchun Chen[1,5], Ming Chen[2] & Meilin Jin[1,5]

[1]State Key Laboratory of Agriculture Microbiology, Huazhong Agriculture University, Wuhan 430070, P. R. China, [2]Department of Bioinformatics, College of Life Sciences, Zhejiang University, Hangzhou, 310058, P. R. China, [3]State Key Laboratory of Crop Genetic Improvement, Center for Bioinformatics, College of Life Science and Technology, Huazhong Agricultural University, Wuhan 430070, P. R. China, [4]Key Laboratory of Horticultural Plant Biology (Ministry of Education), College of Horticulture and Forestry Science, Huazhong Agricultural University, Wuhan 430070, P. R. China, [5]Laboratory of Animal Virology, College of Veterinary Medicine, Huazhong Agriculture University, Wuhan 430070.

Pandemic H1N1/2009 viruses have been stabilized in swine herds, and some strains display higher pathogenicity than the human-origin isolates. In this study, high-throughput RNA sequencing (RNA-seq) is applied to explore the systemic transcriptome responses of the mouse lungs infected by swine (Jia6/10) and human (LN/09) H1N1/2009 viruses. The transcriptome data show that Jia6/10 activates stronger virus-sensing signals, such as the toll-like receptor, RIG-I like receptor and NOD-like receptor signalings, as well as a stronger NF-κB and JAK-STAT singals, which play significant roles in inducing innate immunity. Most cytokines and interferon-stimulated genes show higher expression lever in Jia/06 infected groups. Meanwhile, virus Jia6/10 activates stronger production of reactive oxygen species, which might further promote higher mutation rate of the virus genome. Collectively, our data reveal that the swine-origin pandemic H1N1/2009 virus elicits a stronger innate immune reaction and pro-oxidation stimulation, which might relate closely to the increasing pathogenicity.

A novel, reassorted H1N1 influenza virus outbreak began in early April 2009 (H1N1/2009) in Mexico and then rapidly spread worldwide in human populations, causing the first influenza pandemic of the 21st century[1]. Research reveals that hemagglutinin *(HA)* and polymerase protein 2 (*PB2*) genes play important roles in the efficient transmission of the H1N1/2009 virus in animals[2]. The NA gene originated from Eurasian swine virus also contributes to the efficient respiratory droplet transmission of the H1N1/2009 virus through affecting the release of the viral particles[3]. Although the pandemic H1N1/2009 viruses display an efficient transmissibility that is equal to the seasonal influenza virus, the viruses are not characterized by a high mortality rate in infected people[4,5]. Subsequent laboratory researches also reveal that the patients infected by pandemic H1N1/2009 only develop non-complicated upper respiratory tract symptoms[5]. The data from animal model experiments, including studies in mice and ferrets, demonstrate that the pandemic H1N1/2009 viruses could stably replicate in the lung tissue but do not display high virulence in these animals[6–8].

Analysis of inflammatory reaction in cell lines or in lung tissue infected by pandemic H1N1/2009 shows that although stronger inflammatory reactions are elicited by the H1N1/2009 virus than by the seasonal influenza virus, the reactions are much weaker than the highly pathogenic H5N1 avian influenza virus[9,10]. In the infected human macrophage, the pandemic H1N1/2009 virus does not elicit a "cytokine storm"[11] which is mainly responsible for pathological damage to the infected host cells.

However, during the spread of pandemic viruses in human populations, viruses highly homologous with pandemic H1N1/2009 were isolated from swine herds in different countries, including Canada[12], Thailand[13], China[14] and other countries. These findings indicate that the pandemic H1N1/2009 virus could transmit into swine from people and has already stabilized in swine herds.

In another alarming sign, the pandemic H1N1/2009 virus still undergoes further reassortment in swine. Virus containing *HA* gene originated from H1N1/2009 virus but neuraminidase (*NA*) and the internal genes originated from the European "avian-like" H1N1 and triple-reassortment swine H1N1 respectively was isolated from swine in Hong Kong in 2010[15]. Another reassorted virus containing the internal genes originated from the H1N1/2009

virus; however, the HA and NA genes originated from the swine influenza virus (SIV) (H1N2) was also isolated in pigs in the United Kingdom[16]. These isolates indicate that the pandemic H1N1/2009 viruses stabilized and underwent continuous reassortment in the swine herds. The novel viruses generated by the reassortment of H1N1/2009 with other influenza viruses in pigs will further alter their viral biological properties, affect the ability of swine-to-human or human-to-human transmission and potentially pose a significant threat to public health.

In an epidemiological surveillance of SIV in central China carried out from August 2009 to April 2010, four viruses that are highly homologous with the H1N1/2009 virus were isolated from swine lungs. The four isolates caused mild symptoms with transient body temperature increases in the infected pigs. Meanwhile, two of them (Jia6/10 and 3/10) could cause severe weight loss and mortality in infected mice[14]. Virus A/Liaoning/1/2009 (H1N1) (LN/09) was isolated from the throat swabs of a 27-year old man who displayed mild flu-like symptoms. The sequenced genome of LN/09 (GenBank accession numbers: JX403975-82) displayed high homology with that of pandemic H1N1/2009 virus. In the present study, we showed that the swine-origin H1N1/2009 virus displayed higher pathogenicity than the human-origin H1N1/2009 virus including more severe body weight loss and pathological lung damage as well as higher cytokine expression in infected mouse model. Given that the swine-origin pandemic H1N1/2009 viruses had displayed distinct biological properties and some of them displayed increased virulence as well as the potential for reverse swine-to-human transmission, we chose LN/09 and Jia6/10 to investigate the different pathogenesis and further to study the mechanism involving in the interaction between the human- and novel swine-origin H1N1/2009 isolates and their host.

High-throughput RNA sequencing (RNA-seq) technology has the potential to reveal the alteration dynamics of the pathogen genome itself and the systemic change of host gene expression in the process of infection of pathogens, which could be beneficial to uncover the interaction mechanism and the pathogenesis of pathogens[17,18]. In this study, by using Solexa/Illumina RNA-seq, transcriptome analysis was performed on mouse lung tissues that had been infected by Jia6/10 and LN/09 viruses. Our data revealed the distinct and subtle transcriptome landscape of mouse lung tissue infected by swine- and human-origin pandemic H1N1/2009 viruses. We also sought to obtain valuable information concerning the cellular gene expression patterns affecting lung function, which result in the different consequences for the two viruses.

Results

Increasing pathogenicity of the swine-origin H1N1/2009 virus. To investigate the differences of the pathogenicity of the swine- and human-origin H1N1/2009 viruses, the body weights and the pathological damage of the mice infected by Jia6/10 and LN/09 were determined. As showing in Fig. 1A, the Jia/10 virus caused more significant body weight loss and four (50%) deaths of the infected mice. However, the body weight of the mice infected by LN/09 virus only displayed slight loss upto day 6 and then maintained increase. The virus titers of the Jia6/10 infected mouse lungs were higher than LN/09 infected mouse lungs on both day 3

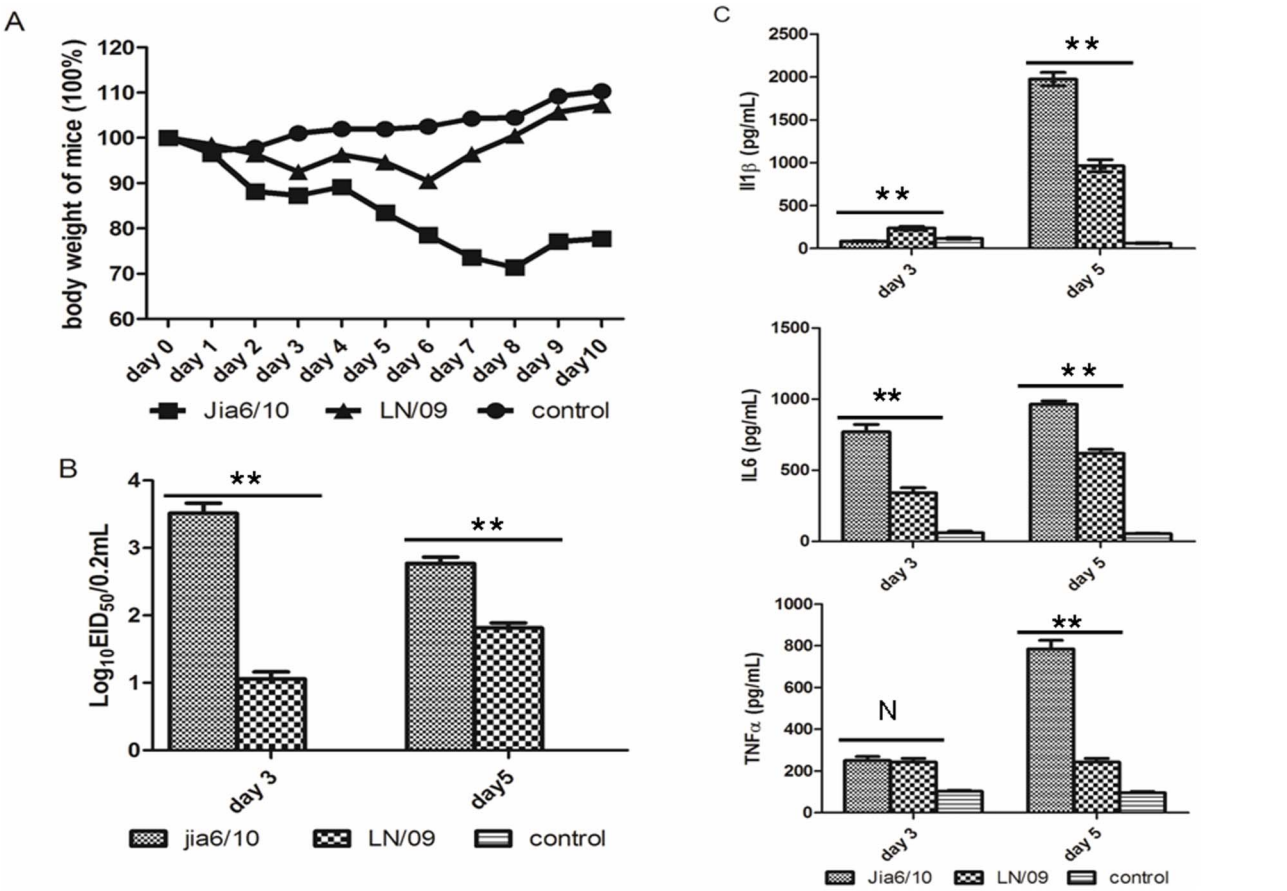

Figure 1 | Pathogenicity of the Jia6/10 and LN/09 viruses in mouse model. (A) Body weight change of the Jia6/10- and LN/09- infected mice from day 0 to day 10; (B) Virus titers of the Jia6/10- and LN/09-infected mouse lung tissues on day 3 and day 5; (C) Expression level of IL-1β, IL-6 and TNFα in Jia6/10 and LN/09 infected mouse lung tissues on day 3 and day 5. **$p < 0.01$, N represents the difference is not significant, and the p values are calculated using the student's t-test.

and day 5 (Fig. 1B). Meanwhile, the mice infected by Jia6/10 developed more severe pathological damage, including necrosis of the alveolar epithelial cells, edema and interstitium broadening as well as infiltration of the inflammatory cells. However, the pathological damages caused by the Jia6/10 and LN/10 viruses were much weaker than that caused by a highly pathogenic H5N1 influenza control (**supplementary figure 1A** [**Supplementary Fig. S1A**]). Furthermore, the Jia6/10 virus stimulated higher expression of IL1β, IL6 and TNFα, indicating that this virus elicited a stronger innate immune reaction in infected mouse lung tissues than LN/09 did (Fig. 1C).

Analysis of the high-throughput sequencing (RNA-seq) transcriptome data. To gain a global and dynamic gene expression profile, RNA-seq was performed to explore the transcriptome of the mouse lung tissues infected by Jia6/10 and LN/09 on day 3 and day 5. More than 206 million 76-bp single-end reads were generated (Table 1). These valuable resources provide information to address two fundamental questions: Which level of the host transcriptome is affected by the virus infection, and what are the main differences in the transcriptome landscape among the samples infected by the two H1N1/2009 viruses?

Generally, approximately 103 million reads could be mapped to the mouse genome, which represented approximately 50% of all the generated reads (Table 1). Of these reads, 94.8% mapped to annotated regions or predicted regions from the public annotation database, and 12.7% spanned exon-exon junctions. Notably, approximately 13.6% of the reads were from pure intronic regions (Fig. 2A). Extensive reads mapping and assembling showed that although the RNA-seq data confirmed 67.2% and 65.6% of the annotated splice junction sites and exons, respectively, a considerable fraction of the detected splice junctions (15.6%) and the assembled exon blocks (24.5%) could not be incorporated into existing gene models (Fig. 2B). Most of these unincorporated junctions (77.7%) and exons (72.9%) overlapped with the annotated gene models, indicating the presence of many unidentified transcript isoforms or natural antisense transcripts; whereas, the rest were mapped to intergenic regions, revealing many putative novel transcribed regions (NTRs) to be identified (Fig. 2B).

To assess the relationship of the whole-transcriptome expression patterns after the lung tissues were infected by the two viruses, a correlation matrix of pairwise comparisons was calculated (Fig. 2C). We found that the two points (day 3 and day 5) of the control and/or the Jia6/10-infected tissues were grouped separately. Notably, the LN/09-treated tissue on day 3 showed a higher correlation with the control group, while LN/09-treated tissue on day 5 was similar to the Jia6/10-infected group; however, the two points of the LN/09-treated tissues were also relatively closely matched (Fig. 2C). Meanwhile, some genome regions showed significant differences between the control and the virus-infected tissues, as exemplified by the local region of the *Serum amyloid A-3* (*Saa3*) gene, which was greatly increased by virus infection. And the expression level of this gene was also different in Jia6/10 and LN/09 infected groups, especially on day 3 (Fig. 2D).

Meanwhile, both viruses activated the production of numerous novel transcribed regions (NTRs) and alternative splicing (AS) events of genes. Notably, most of the NTRs were regulated by the virus infection and demonstrated diversity across the Jia6/10- and LN/09-infected groups (**Supplementary Fig. S2; Table S1 and Supplementary Materials and Results**). In summary, a total of 337 splicing events from 261 genes that changed significantly were identified in the virus-infected groups (false discovery rate (FDR) < 0.05; **Supplementary Table S2**). Notably, a higher frequency of virus-specific AS events was observed in the Jia6/10-infected tissue than in the LN/09-infected tissue on both day 3 and day 5 in all the eight different AS models (**Supplementary Fig. S3A; Table S2 and Supplementary Materials and Results**). Research has proved that a new splice variant of the human guanylate-binding protein 3 (*Gbp3*) gene mediates anti-influenza activity through inhibiting viral transcription and replication[19]. And in this study, we identified the AS transcripts of *Gbp5* gene in both Jia6/10 and LN/09 infected mouse lung tissue (**Supplementary Fig. S3A**). The detailed role of the AS of *Gbp5* gene in the pathogenesis of Jia6/10 and LN/09 infection need further investigation. Since AS plays an important function in inducing the biodiversity of transcriptome and proteome by producing multiple mRNA and protein isoforms with a single gene[20], our results suggested that Jia6/10 exerted a greater influence on the transcriptome or proteome complexity than the LN/09 virus, and the complexity was increasing along the process of virus infection.

Finally, further functional analysis of the genes involved in the virus-infected splicing events with the DAVID program (http://david.abcc.ncifcrf.gov/) revealed that these genes were functionally enriched in different biological processes, including the alternative splicing, acetylation and phosphorylation. Interestingly, some of these genes participated in RNA splicing or RNA processing process, indicating that the virus promotes the RNA complexity in host cells by regulating the splicing regulator during their lifecycle.

Dynamics of the virus-infected mouse transcriptome. To quantify and compare the gene expression level within and between the control and the virus-infected groups, we calculated and normalized the expression level of the genes through reads per kilobase of exon model per million mapped reads (RPKM). Using a threshold of > 1 RPKM in a given sample to define an "expressed" gene, 2,246 genes (12.1%) showed highly differential expression between the control and the virus-infected mouse lungs on both day 3 and day 5 with at least a fourfold change. Interestingly, the numbers of the upregulated genes were larger than the numbers of the downregulated genes in both virus-infected mouse groups at both time points (Fig. 3A; **Supplementary Table S3**). However, the distributions of the downregulated genes were much more diverse than the upregulated genes. Most upregulated genes were enriched in the common set of comparisons, while the downregulated genes were distributed within different single comparison groups (Fig. 3B). Consistent with this observation, the number of overall upregulated genes (1,060) was lower than that of the downregulated genes (1,153). Notably, approximately 100% of the differentially expressed

Table 1 | Statistics of RNA-seq data of the control and the Jia6/10-and LN/09-infected groups

sample	Total reads number	Mapped number (%)	Junction number (%) *
Control 3d (CK3d)	34,768,246	17,437,553 (50.15%)	2,203,535 (12.64%)
Control 5d (CK5d)	36,749,042	17,642,987 (48.01%)	2,036,326 (11.54%)
Jia6/10 3d	35,224,986	14,497,494 (41.16%)	1,844,470 (12.72%)
Jia6/10 5d	31,694,107	19,422,629 (61.28%)	2,461,232 (12.67%)
LN/09 3d	32,563,497	16,735,295 (51.39%)	2,193,341 (13.11%)
LN/09 5d	35,314,944	19,601,355 (55.50%)	2,338,884 (11.93%)
total	206,314,822	105,337,313 (51.06%)	13,077,788 (12.42%)

*Reads were aligned to the mouse genome by Bowtie and Tophat.

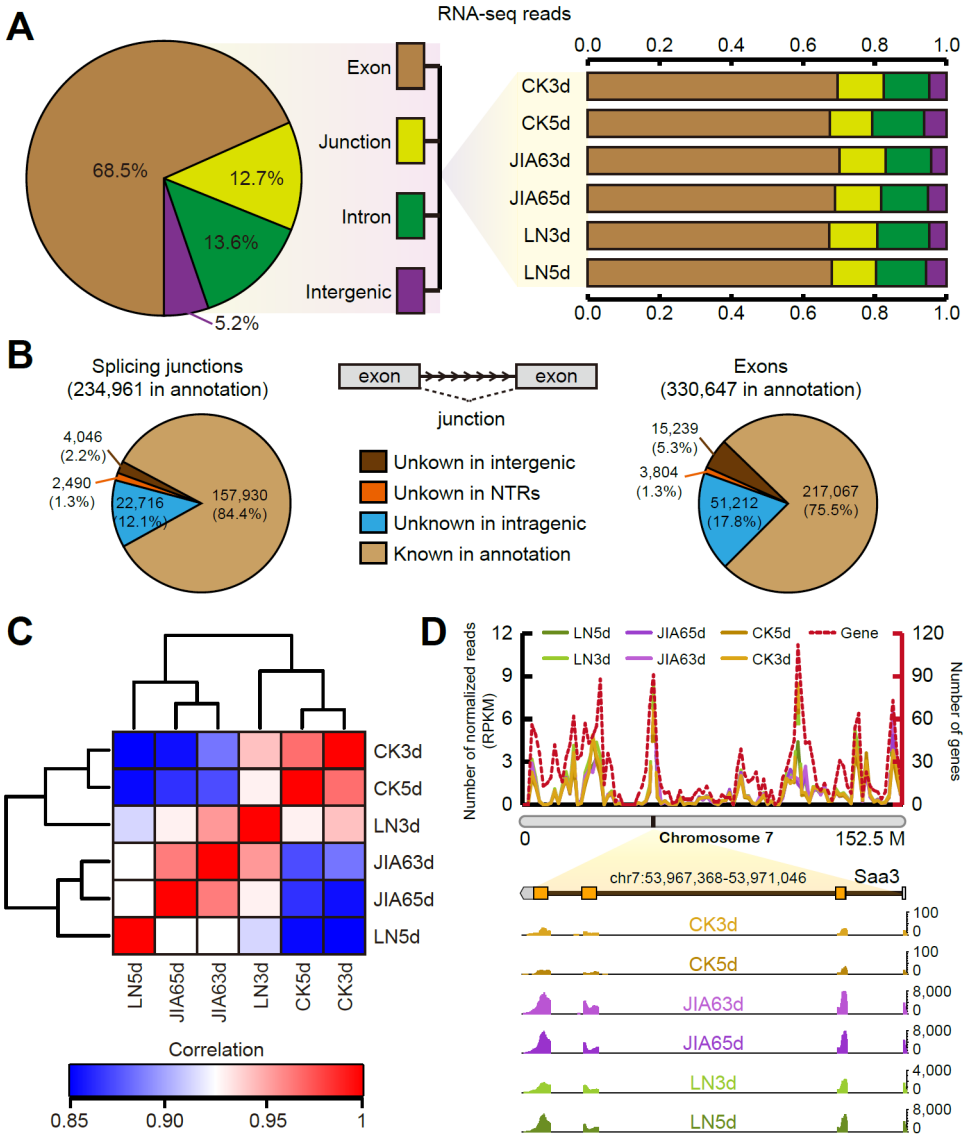

Figure 2 | Global overview of the RNA-seq data of the control and the Jia6/10- and LN/09-infected groups. (A) Pie chart demonstrating the proportion of RNA-seq reads assigned to mice annotated genomic features (left). The distribution of mapped reads from each sample is shown in the right bar chart. CK3d: control 3d group; CK5d: control 5d group; JIA6 3d: Jia6/10-infected 3d group; JIA6 5d: Jia6/10-infected 5d group; LN3d: LN/09-infected 3d group; LN5d: LN/09-infected 3d group; the abbreviation of each group was also used in the subsequent figures. (B) RNA-seq data supporting for known and unknown gene models. Splicing junctions (left) are detected by TopHat and exons (right) are assembled by the Cufflinks program. The junctions and exons are then assigned to existing gene models in annotation or NTRs identified in this study. "Known" suggests that junctions or exons are identical with annotated gene features, while "unknown" means they are not incorporated into existing gene models. A diagram of gene model with two exons and one linked junction is shown in the middle. The numbers of annotated junctions and exons are indicated in parentheses. (C) Heat map matrix of pairwise Spearman correlation between six samples. (D) The distribution of RNA-seq reads (calculated as RPKM) and annotated genes (dashed red line) across the chromosome 7. An example of gene (*Saa3*) induced after virus-infection is shown on the bottom panel.

genes (particularly for the upregulated genes) showed identical expression patterns across all investigated samples (Fig. 3C); with only 33 genes showed mixed expression patterns (Fig. 3D, inserted pie chart). Furthermore, to examine the biological roles of the differentially expressed genes, a Gene Ontology (GO) enrichment analysis was applied to the up- and downregulated genes. Notably, the upregulated genes were mostly enriched in the regulation of immune reactions, such as the immunity system progress, the immune response, the defense response, the innate immune response and the inflammatory response. However, most downregulated genes were involved in the cellular metabolism processes, such as striated muscle contraction, oxygen transport and the regulation of biological reaction (Fig. 3D; **Supplementary Table S4**). The downregulated genes engaged in the regulation of oxygen transport and gas transport indicated that the respiratory and gas metabolism function weakened or were damaged after virus infection, which might be closed related to the pathogenesis of the virus. To directly determine which pathways the two viruses affected after infection, all of the differentially expressed genes were mapped to the entire pathway based on the Reactome database[21]. The upregulated genes were observed largely enriched in the highly connected or pivot nodes in the pathway, while the downregulated genes were distributed at the terminal nodes of gene network. Two of the largest clusters of upregulated gene were found to participate in cell cycle regulation and interferon (IFN) regulation pathways (Fig. 3E).

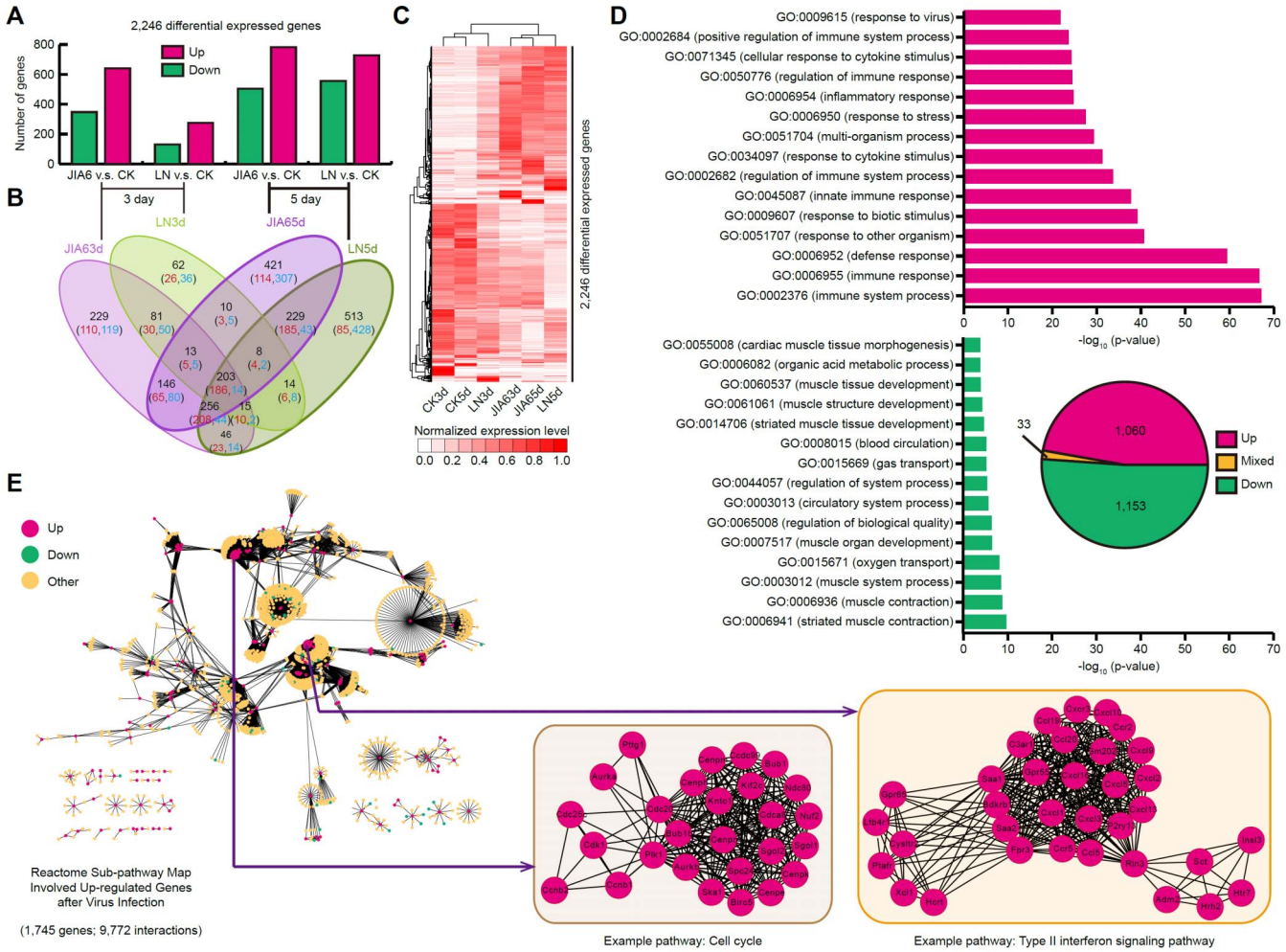

Figure 3 | Analysis of the differential genes and the functional maps of the Jia6/10 and LN/09-infected transcriptome. (A) Differentially expressed genes (with at least a 4-fold change) between control (CK) and virus-infected cells. The number of up- (pink) or down-regulated (green) genes for each comparison are shown in the bar chart. (B) Venn diagram showing the distribution of shared differentially expressed genes (indicated in (A)) among JIA63d, JIA65day, LN3d and LN5d. Gene number is listed in each of the categories. Numbers in parentheses indicate the number of up- or down-regulated gene within each category. Please note that the total number of up- and down-regulated genes in the parenthesis may not be equal to the number of genes in some categories, because some genes showed mixed expression patterns (i.e., up-regulated in one comparison, while down-regulated in another comparison, and vice versa) in the categories. (C) Two-way clustering analysis of all the 2,246 differentially expressed genes. (D) Gene Ontology (GO) enrichment analysis for the up- (top bar chart) and down-regulated genes (bottom bar chart), respectively. Only the top 15 enrichment of GO terms from "biological process" category are listed here. The inserted pie diagram depicts the number of up- and down-regulated or mixed genes. (E) Pathway analysis of differentially expressed genes. All the differentially expressed genes are mapped to the entire pathway based on Reactome. Inserted boxes show the two largest sub-pathways enriched within the up-regulated genes.

Two virus infections impact the cellular innate immunity response through distinct models and with different magnitudes. As mentioned above, although the change in magnitude was not identical, the upregulated genes triggered by the Jia6/10 and the LN/09 infections displayed identical change patterns and were associated with biological functions related to innate immune processes. Therefore, the differences between the innate immune reaction caused by the Jia6/10 and LN/09 infection were comprehensively discussed.

The innate immune system is the first defense of an organism and is associated with a highly conserved host-cell signaling mechanism that protects the host against invading pathogens[22]. Different pattern-recognition receptors (PRRs) are expressed to recognize pathogen-associated molecular patterns (PAMPs), which initiate the signaling cascades inducing the production of proinflammatory cytokines and IFNs[22]. Currently, three types of PRRs have been identified (to be activated in response to viral pathogens infection): the RIG-I like receptors (RLRs), the toll-like receptors (TLRs) and the NOD-like receptors (NLRs). The expression levels of all TLR genes (except *Tlr5*) increased in response to Jia6/10 and LN/09 infection (Fig. 4; **Supplementary Table S3**). Among the different TLRs, TLR3 and TLR7 mainly recognize dsRNA and ssRNA, respectively, which would be produced during influenza virus infection[23,24]. In this study, both Jia6/10 and LN/09 activated the TLR signaling mainly through a Tlr7/Myd88/Irf7-dependent mechanism. Previous study indicated that mice lacking *Tlr7* and *Myd88* fail to induce antiviral protection against influenza virus challenge[25]. Our data showed that the degree of increase of these genes was apparently higher in the lungs of the Jia6/10-infected mice than in the LN/09-infected groups on both day 3 and day 5. The magnitude of the signal activation decreased from day 3 to day 5 in both the Jia6/10- and LN/09-infected mouse groups (Fig. 4). The RLR family, which includes RIG-I, Mda5 and Lgp2. RIG-I and Mda5 could recognize single-stranded 5′-triphosphate RNA with base-paired structures and long dsRNA, respectively[26,27]. The RLR and the TLR signalings sensing influenza virus infection play partially redundant roles in inducing innate immunity[28]. In the

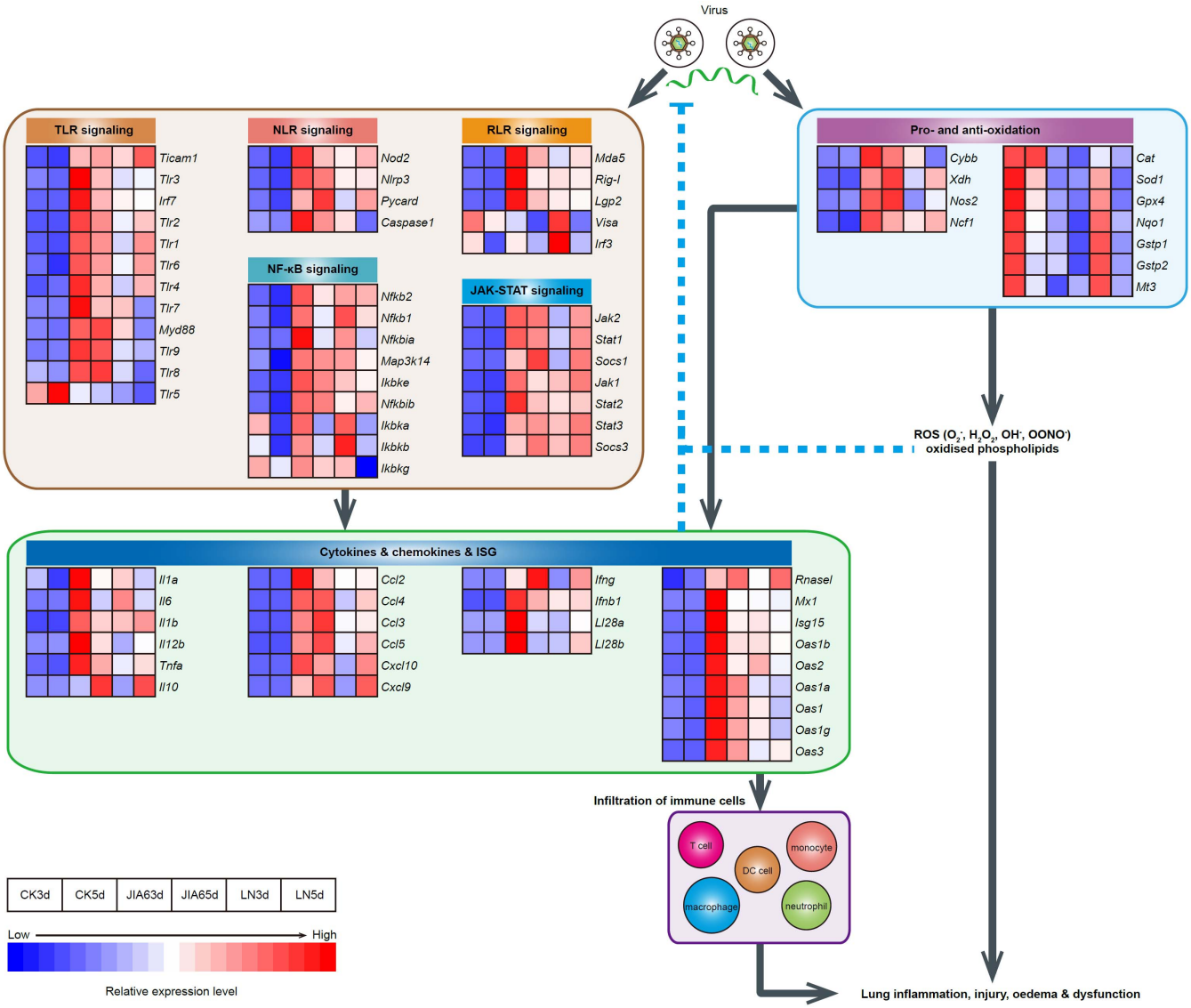

Figure 4 | Comprehensive analysis of the gene expression pattern of the innate immune and oxidation reaction after the Jia6/10 and the LN/09 infection. Genes play significant role in the TLR, RLR and NLR signalings as well as NF-κB and JAK-STAT signalings are included (upper and middle left). The up-regulated genes which encode interleukins, interferons, chemokines and ISGs as well as those associated with influenza virus infection are analyzed (lower left). Genes associated with pro-and anti-oxidation reaction also listed in the figure (right part). The six grids in each line represent the six groups (CK3d, CK5d, JIA63d, JIA6/5d, LN3d and LN5d), and the color in the grid represents the relative expression levels showing in the lower left quarter.

present study, both *RIG-I* and *Mda5* genes were upregulated in the Jia6/10- and LN/09-infected mouse lungs on day 3 and day 5. The expression level of the two genes was higher in the Jia6/10 groups than in the LN/09 groups. Furthermore, the expression level of the two molecules decreased in the Jia6/10-infected mouse lungs but maintained an increased level in the LN/09-infected groups from day 3 to day 5, indicating that the activation of RIG-I and Mda5 did not progress at the same rate during the Jia6/10 and the LN/09 infections (Fig. 4; **Supplementary Table S3**). Meanwhile, a significant activation of *Lgp2*, a negative regulatory gene of RIG-I and Mda5[29], was observed in both the Jia6/10- and the LN/09-infected mouse lungs (Fig. 4). The continuous increase of *Lgp2* from day 3 to day 5 in both the Jia6/10- and the LN/09-infected groups indicated that the organism prevented the excessive production of the downstream inflammatory cytokines by regulating the activation of the RLR signaling. NLRP3, an NLR signal, could form a functional inflammasome complex with PYCARD (its adaptor protein), which responds to external stimuli and plays a role in regulating the activation of capase-1 and the maturation of IL-1b and IL18[30]. In the present study, four members of the NLR signaling group (*Nod2*, *Nlrp3*, *Pyard* and *caspase 1* genes) increased after the Jia6/10 and the LN/09 infections (Fig. 4). Generally, the Jia6/10 virus activated stronger TLR, RLR and NLR signaling reactions than LN/09, which might be associated with the higher pathogenicity of Jia6/10.

NF-κB is a protein complex that controls the transcription of a large number of genes associated with inflammatory cytokines and the downstream interferon-stimulated genes (ISGs)[31]. The expression of *Nfkb1*, *Ikbka*, *Ikbkb* and *Ikbkg* genes in the canonical pathway of NF-κB signaling showed minor changes after infection with both viruses. This result was consistent with the upregulation of the NF-κB inhibitors (*Nfkbia* and *Nfkbib*) after the Jia6/10 and the LN/09 infections (Fig. 4). However, the expression of *Nfkb2* and *Ikbke* genes in the non-canonical pathway of NF-κB signaling increased in both virus-infected groups (Fig. 4), which might suggest that the Jia6/10

and the LN/09 viruses both activated NF-κB signaling, with different magnitudes, through the non-canonical pathway but not through the canonical pathway.

The cytokines and chemokines play significant roles in defending against the virus infection and recruiting inflammatory cells to the infection site. The data revealed that the important pro-inflammatory factor genes (*IL1b* and *IL6*) increased significantly in both virus-infected groups, and the expression values were obviously higher on day 3 than day 5. However, the expressions levels of most chemokines maintained an increase from day 3 to day 5 (Fig. 4; **Supplementary Table S3**). The different trends might relate to the different production processes associated with the pro-inflammatory cytokines and the chemokines after virus infection. Notably, certain chemokines (e.g., *Cxcl10*) significantly increased in response to the Jia6/10 (294-fold on day 3 and 537-fold on day 5) and LN/09 (57-fold on day 3 and 639-fold on day 5) infections. Meanwhile, chemokines *Ccl2*, *Ccl3*, *Ccl4*, *Ccl5*, *Ccl7*, *Cxcl1*, *Cxcl2*, *Cxcl9*, *Cxcl10*, *Cxcl13* and *Cxcl16* were more highly expressed in the Jia6/10-infected groups. The IFNs, e.g., *Ifnb*, *Ifng*, *Il28a and Il28b*, as well as tumor necrosis factor alpha (*Tnfa*), were significantly upregulated in the two virus-infected mouse lungs, particularly the *Ifng* in the Jia6/10 (215-fold) and the LN/09 (152-fold) infection groups on day 5. Notably, the expression of most cytokines and chemokines was higher in the Jia6/10-infected mouse lungs than in the LN/09-infected groups, which indicated that Jia6/10 activated a much stronger inflammatory response and greater inflammatory cell recruitment (Fig. 4; **Supplementary Table S3**).

By binding to the receptor, type I IFN will activate the JAK-STAT signaling pathway and promote the expression of numerous ISGs, which play a significant role in defending against virus infection[32]. In this study, the data showed that the expression of *Jak2*, *Stat1* and *Stat2* genes increased in response to the Jia6/10 and the LN/09 infections. The expression of different types of ISGs, such as *Mx1*, *Isg15* and members of the *Oas* gene family also increased after infection by Jia6/10 and LN/09. Notably, the expression level of most ISGs was higher on day 3 than on day 5 in both the Jia6/10- and LN/09-infected mouse lungs. The expression level was obviously higher in the Jia6/10-infected groups than in the LN/09 groups (Fig. 4; **Supplementary Table S3**). This difference might be associated with the virus replication process and the higher virulence of Jia6/10 in infected mice.

Pro- and anti-oxidation effects elicited by virus infection. The production of reactive oxygen species (ROSs) and reactive nitrogen species (RNSs), particularly superoxide, is an important host defense mechanism for clearing invading pathogens[33]. However, excessive oxidation stress is an important consequence of the immunopathology associated with influenza virus infection[34]. The important pro-oxidation genes, *Cybb*, *Xdh*, *Nos2* and *Ncf1*, which are responsible for generating free radicals, increased in the Jia6/10- and the LN/09-infected mouse lungs on day 3 and day 5. Meanwhile, most anti-oxidation genes, such as *Sod1*, *Nqo1*, *Cat*, *Dhdh*, *Gstp1*, *Gstp2* and *Gpx4*, decreased in both the Jia6/10- and the LN/09-infected mouse lungs (Fig. 4; **Supplementary Table S3**). Overall, the increase in the pro-oxidation factors and the decrease in the anti-oxidation factors were more significant in the Jia6/10-infected groups than in the LN/09 groups, indicating that the Jia6/10 virus stimulated greater ROS and RNS production, which might be associated with its higher virulence in mice.

Meanwhile, the ROS-generated DNA damage presents a significant mutation risk and might accelerate organism evolution[35,36]. In this study, we also mapped the sequencing reads to the genomes of Jia6/10 and LN/09. The results revealed that a total of 29 point mutations occurred in the Jia6/10 virus genome, while the mutation number in LN/09 virus genome was only 19. Six mutations occurred in the HA gene of the Jia6/10 virus; however, no mutation was found in the LN/09 HA gene (**Supplementary Table S5**). Notably, the 6 mutated nucleotides resulted in 5 amino acid mutations, and 2 located at the antigenic site of the HA protein. The high mutation rate of the Jia6/10 genome might relate to the stronger pro-oxidation reaction elicited by the Jia6/10 virus and may partially verify the role of ROS in the promotion of genome mutation.

Discussion

Previous studies have shown that the pandemic H1N1/2009 stabilized in the swine population in different countries[12–14]. The human-to-swine transmission of the pandemic H1N1/2009 virus could substantially affect the evolution and epidemiology as well as the biological properties of the virus. In this study, we have showed that some swine-originated H1N1/2009 viruses displayed increasing pathogenicity compared with the human H1N1/2009 virus. Jia6/10 could cause mortality and significant weight loss of the infected mice without previous adaptation, while the LN/09 virus only raises the transient weight loss after infection. Meanwhile, the Jia6/10 virus results in more severe pathological damage (compared to LN/09) in infected mouse lung tissues. However, the mechanism for the increased pathogenicity after the transmission of pandemic H1N1/2009 to swine and the interaction between swine pandemic H1N1/2009 and the host is still unclear and deserves clarification. In an attempt to reveal the mechanism underlying the increasing pathogenicity after the transmission of pandemic H1N1/2009 to swine, RNA-seq was performed to explore the systemic and subtle transcriptome alterations of the mouse lung tissues infected by the swine and human pandemic H1N1/2009 viruses.

The global transcriptome data showed that the gene expression patterns, for both protein-coding genes and newly identified NTRs, significantly changed after the lung tissue was infected by Jia6/10 and LN/09 viruses. Meanwhile, numerous NTRs and ASs might contribute to the extensive level of transcriptome complexity due to virus infection. Notably, the differential upregulated genes were mainly associated with immune reaction regulation, and the activated innate immunity might be associated with pathological injury to the lung tissue.

Acute lung injury (ALI) is a common consequence of a cytokine storm in the lung alveolar environment and systemic circulation[37]. The balance of pro- and anti-inflammatory mechanisms is critical to maintaining lung immune homeostasis. In the present study, the three innate immunity regulating pathways (TLR, RLR and NLR signalings) and numerous inflammatory cytokines were activated in response to the infection of Jia6/10 and LN/09, particularly on day 3 in the Jia6/10-infected group. All these data showed that the Jia6/10 virus activated a much stronger inflammatory response than LN/09 on both day 3 and day 5. The changing trend of the activated virus-sensing signaling is consistent with the virus titers of Jia6/10- and LN/09 infected mouse lung tissues and the pathogenicity of the two viruses: the higher virulent Jia/10 virus stimulated stronger innate immune signaling on day 3 which in turn inhibited its further replication on day 5, while the lower virulent LN/09 virus stimulated a relatively weak innate immune signaling on day 3 which nearly did not affect its further replication on day 5.

However, when compared with the transcriptome data from the lungs of mice infected with a highly pathogenic H5N1 influenza virus, (A/duck/Hubei/hangmei01/2006 [Hm/06]), which could lead to a cytokine storm and result in severe pathological damage to the lungs[38,39], the expression levels of most chemokines in the Jia6/10 and LN/09 groups were obviously lower than in Hm/06 groups (data not show). Meanwhile, the pathological damage associated with Jia6/10 infection was obviously weaker than that of Hm/06 (Fig. 1), which might indicate that both Jia6/10 and LN/09 didn't promote a cytokine storm in the lungs of infected mice. This observation is consistent with the upregulation of distinctive negative regulatory genes, such as *Tollip, Socs1* and *Socs3*, which involve in inhibiting different

cytokine-induced signaling. Meanwhile, the activated JAK-STAT signaling, as well as the upregulation of ISGs, might play a significant role in restricting virus replication. This indicates that the pathogen-infected tissues are in a state of "high-alert" situation in which the inflammatory reaction can either be efficiently initiated if the infection progresses or prevented if the infection resolves[40].

Apart from stimulating a robust pro-inflammatory response, the virus infection also results in the production of ROSs (O_2^-, OH^-, H_2O_2) and RNS intermediates (nitric oxide (NO), NO_2, HNO_2, $ONOO^-$)[41]. While both ROSs and nitrogen intermediates display potent antimicrobial activity against a variety of pathogens, they can also cause extensive tissue damage if produced in excess[34,41]. Upregulated pro-oxidation genes and downregulated anti-oxidation genes might elicit excessive amounts of ROS and RNS in both Jia6/10 and LN/09 infections. Although the pro-oxidation ability is relatively weaker than the highly pathogenic H5N1 virus hm/06 (data not show), the Jia6/10 virus elicits a much stronger pro-oxidation reaction than LN/09. Previous study has verified that the oxidized phospholipid (OxPL) was produced through TLR4-TRIF-TRAF6 pathway and was able to induce ALI in inactivated H5N1 challenged mice. *Tlr4* silencing could protect mice from H5N1-induced ALI, and inhibiting the expression of *Ncf1*, which regulates the production of ROS, relieves the severity of H5N1-mediated ALI[42]. The results are well consistent with our present observation that the mice infected by Jia6/10 displayed more severe lung damage accompany with higher expression of *Tlr4* and *Ncf1* in this study.

The excessive production of ROS and RNS is harmful to organisms, whereas, they might be beneficial for the mutation of virus genomes, which could produce more virulent and adaptable viruses. This phenomenon might be one of the potential causes of the increasing virulence of the Jia6/10 virus.

A virulent H1N1/2009 virus (MA-CA/04), containing 5 amino acids mutations (G155E, S183P and D222G in HA; E158G in PB2; D101G in NP) was selected through serial lung passage of A/CA/04/2009 (CA/04) in mice[43]. However, none of these sites was found in the mutations of Jia6/10 and LN/09 genome. Interestingly, the original amino acids at site 222 of the HA protein of Jia6/10 and LN/09 viruses were G and D, respectively, indicating the potential high virulence of Jia6/10 virus. Notably, we identified the G222E mutation in the genome of Jia6/10 infected mouse lung tissues, suggesting that the mutation of the virus genome is complex and multi-directional. Further microarray analysis of the mouse lung tissue infected by CA/04 and MA-CA/04 revealed that MA-CA/04 infection was associated with stronger immune response and some of the differential genes enriched in interferon regulatory factor (IRF) binding motif, immune cell trafficking genes including chemokines and their receptor as well as proinflammatory cytokine genes such as *IL6* and *Tnfα*[43]. Most of the differential genes associated with immune response were also identified in Jia6/10 infected mouse lung tissues in the present study. The similar expression pattern of these genes related to immune reaction suggests their important functions in the increasing pathogenicity of the Jia6/10 and MA-CA/04 viruses.

In conclusion, both Jia6/10 and LN/09 elicit a complex cellular response in infected mouse lung tissues. The innate immune response and the pro-oxidation process are activated more significantly on day 3 rather than on day 5 in mouse lungs infected with the swine-origin pandemic H1N1/2009 virus. Although the inflammatory reaction and pro-oxidation are still weaker than those produced by the highly pathogenic H5N1 avian influenza virus and neither virus elicits a cytokine storm, Jia6/10 triggers a stronger inflammatory reaction and pro-oxidation stimulation and higher cytokine production than LN/09. These differences might be closely related to the increasing virulence of Jia6/10. In light of the increase in virulence and the potential for reassortment and reverse swine-to-human transmission, it is essential to investigate the epidemiology and the evolution of the swine-origin pandemic H1N1/2009 virus.

Methods

Pathogenicity of the swine- and human-origin H1N1/2009 viruses. Stock viruses were prepared by propagating the LN/09 and Jia6/10 viruses in MDCK cells at 37°C in a 5% CO_2 incubator. The infectious titers were determined using the Reed and Muench method[44]. Each mouse was infected intranasally with 50 μL of virus stock fluid diluted in PBS to 10^3 $TCID_{50}$. The change of the body weight and the histopathological analysis of the infected mouse lung tissues on day 3 and day 5 were determined after Jia6/10 and LN/09 infection. The production of cytokines IL-1β, IL-6 and TNFα were also detected by enzyme-linked immunosorbent assay (ELISA). The detailed procedures were described in **Supplementary Materials and Results**.

All animal experiments were conducted in compliance with *Guide for the Management and Use of Laboratory Animals* (Hubei province, July, 2005) and the legislation of *Experimental Animal Management Ordinance* (Ministry of S&T of the people's Republic of China, Oct, 1988). The animal studies were approved by Experimental Animal Center, Institute of Medicine, Hubei Province, China (No. 00018734).

RNA preparation and Solexa/Illumina sequencing. Each mouse was infected intranasally with 50 μL of Jia6/10 and LN/09 viruses at 10^3 $TCID_{50}$. On day 3 and day 5, the infected- and control- mouse lung tissues were collected and applied to RNA extraction and Solexa/Illumina sequencing. The detailed procedures and the Solexa/Illumina sequencing were described in **Supplementary Materials and Results** on line.

Bioinformatics analysis. To systematically characterize the transcriptome of virus-infected tissue, we employed various publicly available tools for the mapping, assembly and quantification of transcripts. We also integrated these tools with additional informatics filtering steps to enrich the results for the most robust transcriptome construction. Read alignment and assembly, discovery of splice junctions, identification of NTRs and AS events as well as the quantification of gene expression levels were described in **Supplementary Materials and Results** on line.

1. Fraser, C. *et al.* Pandemic potential of a strain of influenza A (H1N1): early findings. *Science* **324**, 1557–61 (2009).
2. Zhang, Y. *et al.* Key molecular factors in HA and PB2 contribute to the efficient transmission of the 2009 H1N1 pandemic influenza virus. *J Virol* (2012).
3. Lakdawala, S. S. *et al.* Eurasian-origin gene segments contribute to the transmissibility, aerosol release, and morphology of the 2009 pandemic H1N1 influenza virus. *PLoS Pathog* **7**, e1002443 (2011).
4. Garten, R. J. *et al.* Antigenic and genetic characteristics of swine-origin 2009 A(H1N1) influenza viruses circulating in humans. *Science* **325**, 197–201 (2009).
5. Dawood, F. S. *et al.* Emergence of a novel swine-origin influenza A (H1N1) virus in humans. *N Engl J Med* **360**, 2605–15 (2009).
6. Maines, T. R. *et al.* Transmission and pathogenesis of swine-origin 2009 A(H1N1) influenza viruses in ferrets and mice. *Science* **325**, 484–7 (2009).
7. Munster, V. J. *et al.* Pathogenesis and transmission of swine-origin 2009 A(H1N1) influenza virus in ferrets. *Science* **325**, 481–3 (2009).
8. Belser, J. A. *et al.* Pathogenesis of pandemic influenza A (H1N1) and triple-reassortant swine influenza A (H1) viruses in mice. *J Virol* **84**, 4194–203 (2010).
9. Osterlund, P. *et al.* Pandemic H1N1 2009 influenza A virus induces weak cytokine responses in human macrophages and dendritic cells and is highly sensitive to the antiviral actions of interferons. *J Virol* **84**, 1414–22 (2010).
10. Sakabe, S. *et al.* Cytokine production by primary human macrophages infected with highly pathogenic H5N1 or pandemic H1N1 2009 influenza viruses. *J Gen Virol* **92**, 1428–34 (2011).
11. Woo, P. C. *et al.* Cytokine profiles induced by the novel swine-origin influenza A/H1N1 virus: implications for treatment strategies. *J Infect Dis* **201**, 346–53 (2010).
12. Pasma, T. & Joseph, T. Pandemic (H1N1) 2009 infection in swine herds, Manitoba, Canada. *Emerg Infect Dis* **16**, 706–8 (2010).
13. Sreta, D. *et al.* Pandemic (H1N1) 2009 virus on commercial swine farm, Thailand. *Emerg Infect Dis* **16**, 1587–90 (2010).
14. Zhou, H. *et al.* Pandemic (H1N1) 2009 virus in swine herds, People's Republic of China. *Emerg Infect Dis* **17**, 1757–9 (2011).
15. Zhu, H. *et al.* Novel reassortment of Eurasian avian-like and pandemic/2009 influenza viruses in swine: infectious potential for humans. *J Virol* **85**, 10432–9 (2011).
16. Howard, W. A. *et al.* Reassortant Pandemic (H1N1) 2009 virus in pigs, United Kingdom. *Emerg Infect Dis* **17**, 1049–52 (2011).
17. Chang, S. T. *et al.* Next-generation sequencing reveals HIV-1-mediated suppression of T cell activation and RNA processing and regulation of noncoding RNA expression in a CD4+ T cell line. *MBio* **2** (2011).
18. Peng, X. *et al.* Unique signatures of long noncoding RNA expression in response to virus infection and altered innate immune signaling. *MBio* **1** (2010).
19. Nordmann, A., Wixler, L., Boergeling, Y., Wixler, V. & Ludwig, S. A new splice variant of the human guanylate-binding protein 3 mediates anti-influenza activity through inhibition of viral transcription and replication. *Faseb J* **26**, 1290–300 (2012).
20. Nilsen, T. W. & Graveley, B. R. Expansion of the eukaryotic proteome by alternative splicing. *Nature* **463**, 457–63 (2010).
21. Croft, D. *et al.* Reactome: a database of reactions, pathways and biological processes. *Nucleic Acids Res* **39**, D691–7 (2011).

22. Akira, S., Uematsu, S. & Takeuchi, O. Pathogen recognition and innate immunity. *Cell* **124**, 783–801 (2006).
23. Le Goffic, R. *et al.* Detrimental contribution of the Toll-like receptor (TLR)3 to influenza A virus-induced acute pneumonia. *PLoS Pathog* **2**, e53 (2006).
24. Diebold, S. S., Kaisho, T., Hemmi, H., Akira, S. & Reis e Sousa, C. Innate antiviral responses by means of TLR7-mediated recognition of single-stranded RNA. *Science* **303**, 1529–31 (2004).
25. Koyama, S. *et al.* Differential role of TLR- and RLR-signaling in the immune responses to influenza A virus infection and vaccination. *J Immunol* **179**, 4711–20 (2007).
26. Kato, H. *et al.* Differential roles of MDA5 and RIG-I helicases in the recognition of RNA viruses. *Nature* **441**, 101–5 (2006).
27. Loo, Y. M. *et al.* Distinct RIG-I and MDA5 signaling by RNA viruses in innate immunity. *J Virol* **82**, 335–45 (2008).
28. Le Goffic, R. *et al.* Cutting Edge: Influenza A virus activates TLR3-dependent inflammatory and RIG-I-dependent antiviral responses in human lung epithelial cells. *J Immunol* **178**, 3368–72 (2007).
29. Rothenfusser, S. *et al.* The RNA helicase Lgp2 inhibits TLR-independent sensing of viral replication by retinoic acid-inducible gene-I. *J Immunol* **175**, 5260–8 (2005).
30. Thomas, P. G. *et al.* The intracellular sensor NLRP3 mediates key innate and healing responses to influenza A virus via the regulation of caspase-1. *Immunity* **30**, 566–75 (2009).
31. Kopp, E. B. & Ghosh, S. NF-kappa B and rel proteins in innate immunity. *Adv Immunol* **58**, 1–27 (1995).
32. Schindler, C. & Plumlee, C. Inteferons pen the JAK-STAT pathway. *Semin Cell Dev Biol* **19**, 311–8 (2008).
33. Schwarz, K. B. Oxidative stress during viral infection: a review. *Free Radic Biol Med* **21**, 641–9 (1996).
34. La Gruta, N. L., Kedzierska, K., Stambas, J. & Doherty, P. C. A question of self-preservation: immunopathology in influenza virus infection. *Immunol Cell Biol* **85**, 85–92 (2007).
35. Ford, C. B. *et al.* Use of whole genome sequencing to estimate the mutation rate of Mycobacterium tuberculosis during latent infection. *Nat Genet* **43**, 482–6 (2011).
36. Belenky, P. & Collins, J. J. Microbiology. Antioxidant strategies to tolerate antibiotics. *Science* **334**, 915–6 (2011).
37. Rubenfeld, G. D. *et al.* Incidence and outcomes of acute lung injury. *N Engl J Med* **353**, 1685–93 (2005).
38. Zou, W. *et al.* Proteomics analysis of differential expression of chicken brain tissue proteins in response to the neurovirulent H5N1 avian influenza virus infection. *J Proteome Res* **9**, 3789–98 (2010).
39. Zou, W., Yu, Z., Zhou, H., Tu, J. & Jin, M. Genetic characterization of an H5N1 avian influenza virus with neurovirulence in ducks. *Virus Genes* **38**, 263–8 (2009).
40. Pothlichet, J., Chignard, M. & Si-Tahar, M. Cutting edge: innate immune response triggered by influenza A virus is negatively regulated by SOCS1 and SOCS3 through a RIG-I/IFNAR1-dependent pathway. *J Immunol* **180**, 2034–8 (2008).
41. Akaike, T. *et al.* Pathogenesis of influenza virus-induced pneumonia: involvement of both nitric oxide and oxygen radicals. *Proc Natl Acad Sci U S A* **93**, 2448–53 (1996).
42. Imai, Y. *et al.* Identification of oxidative stress and Toll-like receptor 4 signaling as a key pathway of acute lung injury. *Cell* **133**, 235–49 (2008).
43. Josset, L. *et al.* Implication of inflammatory macrophages, nuclear receptors, and interferon regulatory factors in increased virulence of pandemic 2009 H1N1 influenza A virus after host adaptation. *J Virol* **86**, 7192–206 (2012).
44. Reed, L. & Muench, H. A simple method of estimating fifty percent endpoints. *Am.J.Hyg* **27**, 5 (1938).

Acknowledgements

This work is supported by China National Basic Research Program (China "973" Program 2011CB505004) and Chinese Postdoctoral Science Foundation (52201-12981). And we thank Master Jianjiang Ke for his help in the management of animal experiments. The high-throughput sequencing is performed in Shanghai Biotechnology Co., Ltd (Shanghai, China).

Author contributions

Z.W., Ch.H. and J.M. designed the experiments; Z.W., Z.J., L.X., Zh.J. performed the animal experiments; Ch.D., X.M., W.L., Ch.L., Zh.H., Ch.M. performed the bioinformatics analysis of the transcriptome data; Ch.D. drew the figures of the manuscript; Z.W., Ch.D., X.M. and J.M. analyzed the data and wrote the manuscript.

Additional information

Supplementary information accompanies this paper at http://www.nature.com/scientificreports

Competing financial interests: The authors declare no competing financial interests.

How to cite this article: Zou, W. *et al.* Insights into the increasing virulence of the swine-origin pandemic H1N1/2009 influenza virus. *Sci. Rep.* **3**, 1601; DOI:10.1038/srep01601 (2013).